Nano Research 2013, 6(5): 303–311
DOI 10.1007/s12274-013-0303-0
Research Article

ISSN 1998-0124
CN 11-5974/O4

Bottom-up synthesis of ultrathin straight platinum nanowires: Electric field impact

Alexander Nerowski[1], Joerg Opitz[1,2], Larysa Baraban[1] (✉), and Gianaurelio Cuniberti[1,3]

[1] *Institute for Materials Science and Max Bergmann Center of Biomaterials, Dresden University of Technology, Dresden 01062, Germany*
[2] *Fraunhofer Institute for Non-Destructive Testing, Dresden 01109, Germany*
[3] *Division of IT Convergence Engineering, POSTECH, Pohang 790-784, Republic of Korea*

Received: 28 January 2013
Revised: 8 March 2013
Accepted: 10 March 2013

KEYWORDS

bottom-up growth,
directed electrochemical nanowire assembly (DENA),
metal nanowires,
nanostructuring,
nanoelectronics,
local electric field

ABSTRACT

We present a study of the electric field effect on electrochemically grown ultrathin, straight platinum nanowires with minimum diameter of 15 nm and length in the micrometer range, synthesized on a silicon oxide substrate between metal electrodes in H_2PtCl_6 solution. The influence of the concentration of the platinum-containing acid and the frequency of the applied voltage on the diameter of the nanowires is discussed with a corresponding theoretical analysis. We demonstrate for the first time that the electric field profile, provided by the specific geometry of the metal electrodes, dramatically influences the growth and morphology of the nanowires. Finally, we provide guidelines for the controlled fabrication and contacting of straight, ultrathin metal wires, eliminating branching and dendritic growth, which is one of the main shortcomings of the current bottom-up nanotechnology. The proposed concept of self-assembly of thin nanowires, influenced by the electric field, potentially represents a new route for guided nanocontacting via smart design of the electrode geometry. The possible applications reach from nanoelectronics to gas sensors and biosensors.

1 Introduction

The fast development of nanofabrication techniques opens new routes for smart design of sophisticated nanoscale devices with unique functionalities [1, 2]. In contrast to well-refined top-down methods like etching, nano-printing or electron beam structuring, an alternative bottom-up concept, based on the production of nanostructures starting at the atomic or molecular level, is in the stage of active exploration [3–6]. The bottom-up approach offers a cost-efficient solution for future electronics as it relies on low material consumption, while avoiding the use of expensive nanolithography techniques [7].

Metallic bottom-up one-dimensional nanostructures have already found applications as elements of ultra-sensitive gas and bio-sensors, or for plasmonics [8–11]. The nanowires can be quickly grown with any aspect

Address correspondence to larysa.baraban@nano.tu-dresden.de

ratios, in a time frame from seconds up to few minutes, which represents a major improvement compared to time consuming conventional lithography [12].

One of the major challenges existing in the field of bottom-up nanowires is to integrate them into circuits. In order to solve this issue, several recently proposed methods involve dielectrophoresis (DEP), the movement of a neutral, polarizable object due to a spatially inhomogeneous electric field [13]. For instance, combination of DEP with directed fluid flow can also be employed for the guidance of nanowires between electrodes in solution [14, 15]. Hermanson et al. have realized the growth of microwires directly from metallic clusters in solution using DEP, which has the advantage that the wires are directly connected [16]. Subsequently, the method was employed to grow nanowires from neutral molecules [17]. Also semiconducting clusters can be arranged in this way, which opens up the application of dielectrophoretically grown wires to field-effect sensing [18]. On the other hand, nanowires can be grown via assembly of charged metallic complexes, using directed electrochemical nanowire assembly (DENA) [19]. Despite the relative simplicity of both methods, full control over the straightness, diameter, and branching of the grown nanowires has not been achieved so far. Several suggestions to optimize the process parameters for both DENA and DEP have been made [20]. Bhatt et al. found that adding a high-viscosity substance to a nanocluster-containing medium increases the straightness of the microwires [21]. The diameter and branching of the nanowires grown using either the DEP or the DENA approach, can be manipulated by changing the parameters of the applied electric signal, e.g., amplitude and frequency [22, 23].

To our knowledge, the growth of nanowires with diameters thinner than 100 nm with simultaneous control of straightness and branching, has not been demonstrated so far, using either DENA or DEP techniques. However, both reported methodologies are particularly promising to make the bottom-up method appropriate for applications in nanoelectronics, e.g., interconnects.

Here, we go beyond previously reported protocols of metal nanowires fabrication and present a controlled method to produce ultrathin, straight, unbranched nanowires with diameters down to 15 nm, using DENA. Furthermore, we demonstrate on a proof-of-concept level the possibility to contact such wires in a nanocircuit, using two-step lithography. Finally, we discuss the influence of the geometry of the metal electrodes and the resulting electrical field profile on the straightness of the wires, which is a crucial point in the design of bottom-up nanowire circuits.

2 Experimental

The electrode fabrication was done on a piece of silicon wafer with a 300 nm oxide layer in the manner as in previous experiments [12], except for the exposure. This step was made with laser lithography (DWL66fs, Heidelberg Instruments) with a 4 mm write-head. The wavelength of the laser was 405 nm. The electrodes were contacted with a tip-probing station (Karl Suss). The electrical signal was provided by a function generator (Tektronix AFG320) and observed by an oscilloscope (Tektronix TDS3014). Figure S1 in the Electronic Supplementary Material (ESM) contains data about the equivalent circuit of the setup. The solution was diluted with deionized water from a bought H_2PtCl_6 stock-solution (Sigma Aldrich 8 wt.%) until a concentration of 200 μM was reached. Since with increasing pH the solution becomes unstable, the experiments were conducted within a maximum of 3 hours after dilution [24]. A drop of 1.5 μL of the diluted solution was put onto the electrodes and a square-shaped signal with a frequency of 500 kHz and peak-to-peak amplitude of 18 V_{pp} was applied, if not stated otherwise. After a growth time of 5 min, the function generator was switched off. The nanowires, grown at room temperature, were characterized using scanning electron microscope (Philips).

3 Results and discussion

3.1 Growth of platinum nanowires

The growth of thin platinum (Pt) nanowires was carried out following a procedure initially demonstrated by Kawasaki et al. [25]. However, we employed a dilute 200 μM aqueous solution of hexachloroplatinic acid (H_2PtCl_6), which is substantially lower than the

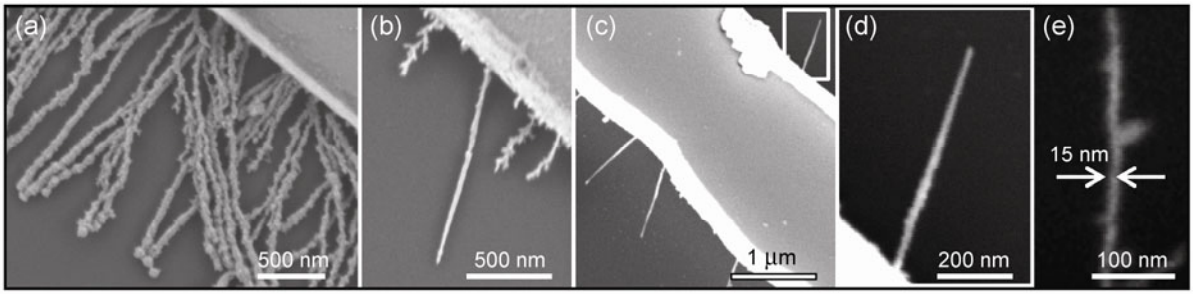

Figure 1 SEM-images of Pt nanowires grown from acidic solution at different frequencies with different corresponding diameters: (a) 60 nm at 100 kHz; (b) 30 nm at 300 kHz; (c), (d) 20 nm at 500 kHz (panel (d) is the magnification of the white square in panel (c)); (e) 15 nm at 1 MHz. Growth of the wires starts at lithographical electrodes immersed in solution.

previously reported concentrations. The solution was put onto a piece of silicon wafer with lithographically fabricated gold microelectrodes. In our experiments we use an electrode geometry where working and counter electrode oppose each other tip-to-tip (see Fig. S2 in the ESM). Figure 1 displays the scanning electron microscopy (SEM) images of thin and unbranched wires, which can be reproducibly fabricated applying an AC square-shaped signal to the electrodes in the frequency range between 100 kHz and 1 MHz. The resulting diameters of the grown Pt nanowires decreased from 60 nm at lower frequencies, down to 15 nm at higher frequencies. This trend is in qualitative agreement with previous works reporting on nanowire growth in an AC electric field [23, 25]. Ultimately, thin nanowires of about 15 nm in diameter could be obtained by applying a square-shaped AC voltage at 1 MHz, which is a factor of ~20 thinner than previously reported values [25]. Since we use low concentrations of hexachloroplatinic acid (a hundred times lower than previously reported), we propose that the mechanism of nanowire assembly in our experiments involves a transition from the reaction-limited regime to the diffusion-limited regime. In dendritic solidification theory, the diameter d_w of the grain, solidified from the liquid, depends on several factors: $d_w = 2\sqrt{2DtSt}$, where D is the diffusion coefficient of the charged particles in solution, St the Stefan number (a measure of the degree of undercooling of a liquid), and t the time of deposition [26]. The equation can be rewritten as:

$$d_w = \frac{2\sqrt{2DSt}}{\sqrt{f}} \quad (1)$$

where f is the frequency of the applied voltage. The diffusion coefficient D can be calculated from the Stokes–Einstein equation $D = k_B T / 3\pi\eta d_p$, where k_B is the Boltzmann constant, T is the temperature, η is the viscosity of the liquid at room temperature, and d_p is the particle diameter. The diameter of a $PtCl_6^{2-}$ ion including its hydrate shell is $d_p \approx 1$ nm [27]. Since the water molecules are much smaller than the dissolved ions, the laws for macroscopic friction may be applied in good approximation [28]. The viscosity of a solution at room temperature can be estimated to be $\eta \approx 1$ mPa·s, as long as the solution contains predominantly water (down to a fraction of about 90 wt.%), which is a condition well met in DENA experiments [29]. Inserting these values, one estimates the diffusion coefficient of charged species in solution as $D = 6 \times 10^{-10}\ m^2/s$ The Stefan number St in turn depends on the bulk concentration of negatively charged ions in solution c_0, the interfacial concentration of negatively charged ions at the liquid interface c_l, and the partition coefficient k (between 0 and 1): $St = (1 - c_0/c_1)/(1-k)$. The ratio of the bulk concentration to the interfacial concentration at the liquid interface $\alpha = c_0 / c_1$ is strongly dependent on the reaction kinetics of the nanowire growth. In the case of a very high bulk concentrations c_0, the reaction at the tip surface is slow compared to the flux of arriving metal complexes, which results in their accumulation at the tip surface (reaction-limited case) [12]. A small value of α results in a high Stefan number St and thus a larger diameter of the nanowires. In contrast, lower bulk concentrations of the charged species c_0, decrease the accumulation of the metal complexes, and at a certain point brings α close to 1. This considerably decreases the Stefan number St, which corresponds to growth kinetics between reaction limitation and

diffusion limitation. We propose that in our experiments c_1 and c_0 are on the same order of magnitude, which leads to a reduction of the diameter of the assembled nanowires. In Fig. 2 we plot measured data of the nanowire diameter versus frequency of the applied AC voltage (red data) grown at a concentration of 200 μM chloroplatinic acid.

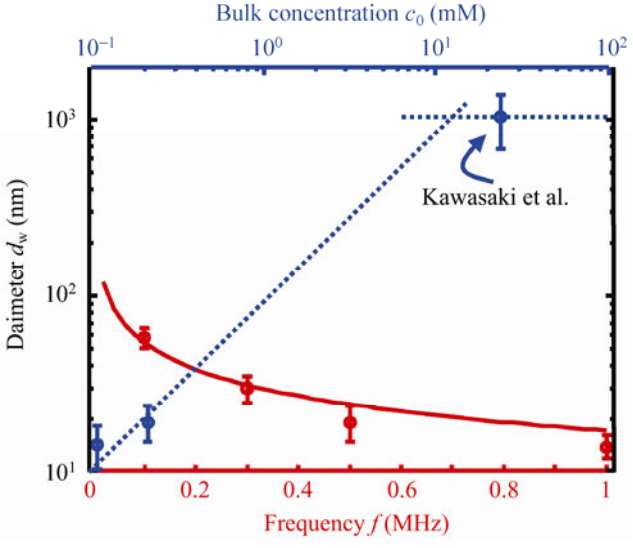

Figure 2 Dependence of the nanowire diameter on frequency and concentration. The red solid line is a fit to the measured data and the blue dotted line is a guide to the eye. The data point at 24 mM is taken from Kawasaki et al. [25].

Each data point represents the average and its standard deviation from six values in total, taken from three different wires grown at the same conditions. The red solid line displays a fit to Eq. (1), and with the above calculated diffusion coefficient D, we have a Stefan number of $St = 0.064$. The ratio of the bulk concentration to the interfacial concentration at the liquid interface α is large ($\alpha \to 1$), which means that there is an accumulation of platinum complexes around the nanowire's tip which just exceeds the bulk concentration. This occurs during the transition from reaction-limitation to diffusion-limitation, as discussed above. This statement is supported by a comparison of the diameters of the nanowires grown at low bulk concentrations 100 μM and 200 μM, to the values obtained for high concentration $c_0 = 24$ mM, as taken from the literature (blue points) [25]. Obviously, at high bulk concentrations, the ratio and thus the diameter does not change substantially, once the reaction-limited regime is reached. The behavior of the Stefan number in between these two kinetically different regimes is more complex, since the partition coefficient k can also increase with the growth velocity (which increases with the bulk concentration) [30]. This phenomenon requires further analysis, therefore the dotted blue line in Fig. 2 is only a guide to the eye, yet appropriate as a qualitative statement. The morphology of the wires grown at 0.1 mM is no different to that of the wires grown at 0.2 mM at the same frequency.

Figure 1 shows that thin, straight and unbranched nanowires can be grown at the sides of the electrodes. The side-growth can be activated by control of the nucleation density, i.e., the number of wire nucleation centers per unit electrode length, which in turn is influenced by various factors. First, geometrical inhomogeneities of the electrode, at which a high electrical field occurs, can facilitate the reduction of metal complexes. Second, the concentration of platinum-containing complexes in aqueous solution also changes the nucleation density, which was recently found confirmed by experiments performed with K_2PtCl_4 salt solution [12]. Finally, an increase of the magnitude of the applied voltage leads to higher nucleation density. Moreover, the applied voltage also has influence on the extent of the nanowire branching [25]. By carefully balancing these three aforementioned parameters straight wires start to grow at the side of the electrodes. The optimal process parameters for our electrode setup were found to be a peak-to-peak voltage of 16–18 V_{pp} at a concentration of 200 μM. To rule out any influence on straightness and branching coming from either the substrate (e.g., by surface roughness) or the electrode material (different lattice constants at the contact site) we conducted the same experiments for a different substrate (glass instead of SiO_2) and/or a different electrode material (Pt instead of Au), yet, achieved the same results.

A physical model for the growth of nanowires is presented in Fig. 3. Since the solution we use is acidic (pH ≈ 3.4), we assume that the majority of the platinum complexes in the solution are $PtCl_6^{2-}$, $PtCl_5(H_2O)^-$ and $PtCl_5(OH)^{2-}$, which are negatively charged [24]. The growth process in the AC field comprises two phases: in the positive half-wave (cf. Fig. 3(a)), the negatively

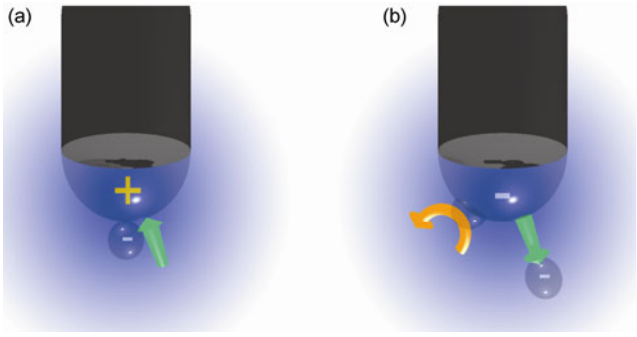

Figure 3 Schematics of the nanowire growth process: (a) Attraction of negatively charged metal complexes; (b) repulsion (green arrow) and reduction (orange arrow) of metal complexes. A high potential/time slope is prerequisite to growth.

charged metal complexes are attracted and accumulate around the tip. In the negative half-wave (see Fig. 3(b)) the complexes are repelled and reduced. Reduction only takes place for those complexes which are still in close vicinity to the nanowire tip, when the reduction potential is reached. For a low voltage/time slope, the complexes are too far off the tip when the reduction potential is reached. For a high slope, the reduction potential is reached when some complexes are still at the tip and reduction takes place. Thus, a high voltage/time slope is indispensible for growth. The described model is in qualitative agreement with previously reported results: growth of the nanowires in an $In(CH_3COO)_3$ solution, with an applied sine wave (low slope) was only possible at very high voltages (>40 V_{pp} @ 1 MHz) [31]. In our own experiments again with H_2PtCl_6 we observed no growth with a sine wave at 500 kHz, but we did observe growth at 10 MHz (always at 18 V_{pp}). A high-frequency sine possesses a high voltage/time slope too, therefore nucleation took place. Experiments performed with an applied AC square-shaped signal (high slope) resulted in successful nanowire assembly in a wide frequency range (down to 10 kHz). Note also the general trend that lower frequencies produce rougher nanowires, because of the longer duration of the half-waves of the electrical signal. The longer attraction phase (positive half-wave) causes a greater accumulation of platinum around the nanowire. In the deposition phase (negative half-wave), occasionally platinum species attach to the sides of the wire, because the platinum species did not all leave the wire surface until the reduction potential was reached.

3.2 Influence of the electrical field on the morphology of the nanowires

Connecting the wires to the circuit can be conventionally performed by growing nanowires between the electrodes. However, this process can lead to a number of undesirable effects. First, upon contact, the current through the wire suddenly increases and can burn the wire. For thicker wires this could be overcome by monitoring the current through the electrodes and switching off the voltage source upon increase. Second, the wire morphology is strongly dependent on the electrical field surrounding the nanowire. Figure 4(a) shows the ground electrode (starting point of the growth) and an electrode with floating potential next to it (floating electrode).

The wires directed into the free space, i.e., with no opposing electrode grow straight and without branches. The wires directed towards the floating electrode reveal a more curved geometry. In order to understand the electric field impact on the nanowires morphology we performed COMSOL simulation, solving the 2D-Poisson equation. Figure 4(b) shows the results of a 2D-simulation of the electrode geometry with two wires with 20 nm in diameter and 1 μm in length. The wires emerge from the ground electrode, where one is directed towards the floating electrode and the other one towards free space (as in panel (a)). Another electrode opposing the ground electrode carries a voltage of 10 V (not shown in the figure). The full electrode geometry can be seen in Fig. S2 in the ESM and is the same as in the experiment in panel (a). The boundary condition at the edge of the floating electrode served the 2D-Maxwell law for the electrical flux $\int_S \rho_S \mathrm{d}S = Q_0$, where S is the electrode surface, ρ_S the charge density and Q_0 the charge of the electrode. The tips of the two wires exhibit the highest electrical field. However, the field at the tip of the wire pointing towards the floating electrode is approximately one order of magnitude higher than at the tip of the other wire. We interpret this result as the consequence of the charge accumulation at the edge of the floating electrode due to the external field. This causes electrical induction and raises the electrical field in between the two electrodes. The global field enhancement is reduced when moving the electrodes further away

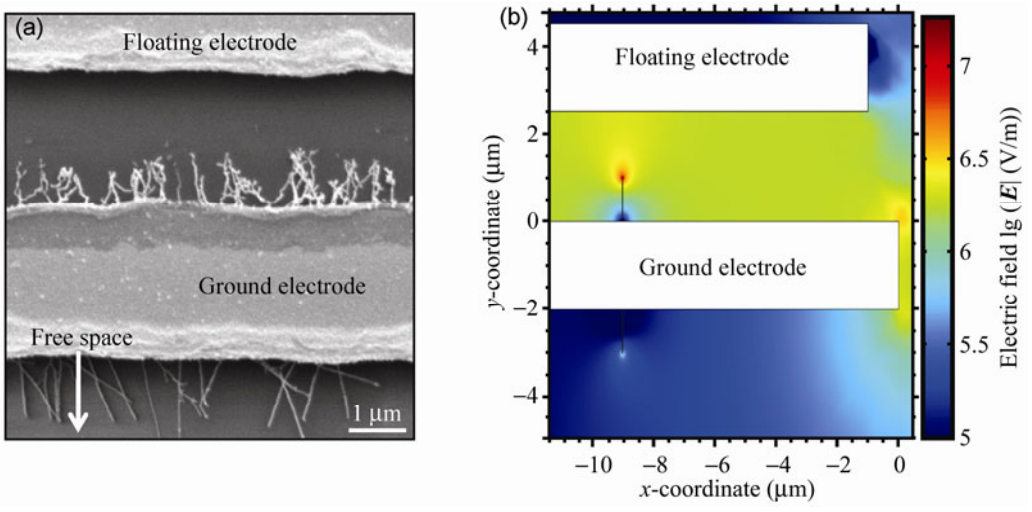

Figure 4 (a) Nanowires growing towards free space exhibit straighter growth than when growing towards another electrode. (b) COMSOL simulation of the electrical field at the electrode geometry and nanowires of 20 nm thickness. One wire points towards an electrode with floating potential and another one to free space. The potential of the working electrode (see Fig. S2 in the ESM for the design) opposing the ground electrode was set to $V = 10$ V. The different lengths of the electrodes serve to ensure that only side-grown wires contact.

from each other, which leads to the straighter wires. Furthermore, the electrical field can be decreased by reducing the magnitude of the applied voltage. However, the nucleation density then decreases until no wires grow at the threshold potential, which is different from the reduction potential and explained in more detail by Ranjan et al. [32] or Lumsdon et al. [33]. In our experiments the threshold voltage is at 14 V_{pp}, which is too high to achieve completely straight wire growth for narrow gaps (<1.5 μm).

It is important to note that high electrical field does not guide the wire but rather disturbs its deterministic one-dimensional growth. For straight wire growth, the electric field serves as electron donor at preferred crystal facets but does not direct the growth of the wire. For dendritic wires, the field forces deposition of Pt at other facets than the energetically preferred ones. Furthermore, the impact of the electric field is found to be crucial for the morphology of ultrathin nanowires, because small curvatures exhibit large electric fields and small defects in the wire structure can disturb the straightness of the wires more easily.

3.3 Towards nanoelectronics: Contacting the nanowires

To contact thin nanowires, like those shown in Fig. 1, it is desirable to neither melt the wires nor to impede their straightness. Due to the above mentioned issues for thin wires, contacting cannot be achieved with a simple two-electrode design, in which the nanowires grow from tip to tip (see Fig. S3 in the ESM). We propose to solve this using two-step lithography, as it is illustrated in Fig. 5. We first grow nanowires at the sides of two gold electrodes, one of which is ground and the other one carries a potential (see Fig. 5(b)). The wires in Fig. 5 were grown at 500 kHz, however, for contacting purposes the wires had to be longer than the ones in Fig. 1. Therefore, we increased the growth time to ~15 min, which caused partial evaporation of the solution drop on the electrodes. This raised the platinum concentration which in turned caused thicker wires (see Fig. 2). We chose not to increase the volume of the drop, since we did not want to change any other setup parameters. The length of the wires depends on the growth time and the growth velocity. The latter in turn depends on several parameters, such as metal concentration, concentration of electrolytes, solution age, temperature of the substrate and frequency of the applied signal [12, 23]. Despite a large variety of influencing parameters, we demonstrate that it is possible to grow wires similar in length and diameter. After the growth process is finalized, a second lithography

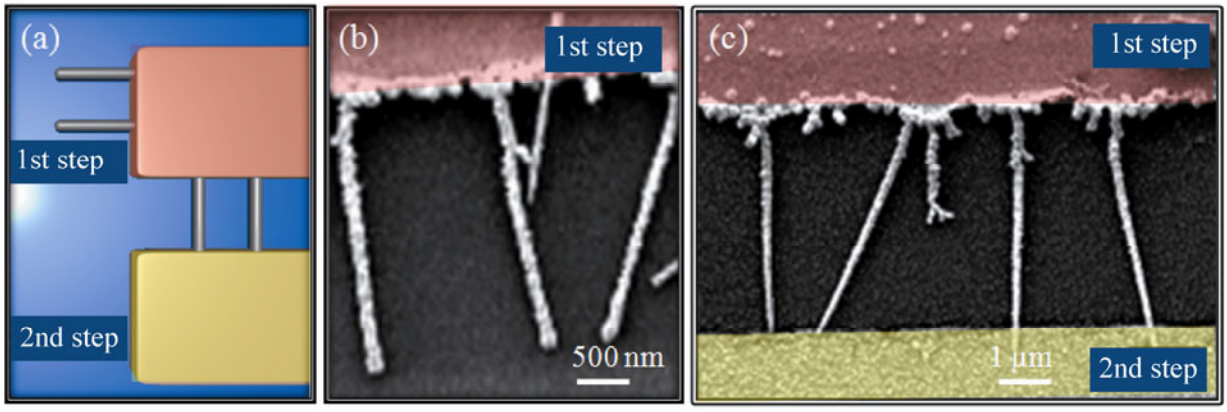

Figure 5 (a) Scheme for contacting ultra thin, straight nanowires. After the first lithography step, the wires are grown at both sides. The second lithography step serves to contact the side-grown wires. (b) SEM-images after the first lithography step. (c) Image of contacted, straight nanowires after second lithography step. Geometrical inhomogeneities in the electrode design were used to initiate wire growth at defined places.

step was performed to contact the nanowires. The alignment was done using a scanning laser lithography setup; however our method can be also applied to UV or e-beam based techniques. Figure 5(c) shows perfectly straight wires, contacted by two electrodes. Note that the wires had to undergo the full lithography process again without being damaged, which hints at an enormous mechanical stability.

4 Conclusions

We demonstrated the growth of ultrathin (down to 15 nm), straight and unbranched Pt nanowires, grown by the DENA process. We emphasize that careful adjusting of three factors, i.e., concentration, voltage and metal electrode geometry, is necessary to achieve a controllable morphology of the nanowires. A crucial factor for decreasing the nanowire diameter is the concentration of the metal complexes in solution. We attribute this phenomenon to the stability of the nanowire tip diameter, theorized by dendritic solidification. Based on experimental facts, we suggest a physical picture of the wire growth. It was shown that the electric field can tremendously disturb the nanowire straightness. As a consequence, an important engineering guideline for nanowire growth is that the applied field should be just low enough that the threshold potential can be reached. Going far beyond the threshold potential can introduce branches and impede the straightness. Furthermore we showed the possibility to deposit wires at electrode inhomogeneities and how to contact the grown wires, which is a step forward towards defined bottom-up nano-circuits.

Note that the parameters of an applied AC electric field make a crucial impact on the structural properties, i.e., diameter, branching, electronic properties, etc., of the grown nanowires. Ongoing investigations of the nanowires crystalline structure reveal an intriguing dependence of the growth morphology on the DENA parameters.

The observed electric field influence on the directionality and morphology of the nanostructures could potentially be used to guide the growth of the nanowires in a deterministic way via providing smart electric field configurations to build up novel nanocircuitry. Moreover, the high surface-to-volume ratio and the better electrical transport characteristics provided by the low diameter of the nanowires likely can boost the sensitivity of nanoscaled gas or biosensors, e.g., hydrogen or glucose sensors [10]. Since the nanowires are already contacted, the packaging into an electrical sensor system is extremely facilitated.

Acknowledgements

This work was supported by the European Union (European Social Fund and European Regional Development Fund) and the Free State of Saxony

(Saechsische Aufbaubank) in the young researcher group InnovaSens (SAB No. 080942409), and by the World Class University (WCU) program through the Korea Science and Engineering Foundation funded by the Ministry of Education, Science and Technology (project No. R31-2008-000-10100-0). We gratefully acknowledge support from the German Excellence Initiative via the Cluster of Excellence EXC 1056 "Center for Advancing Electronics Dresden" (cfAED). We thank M. Poetschke and M. Bobeth for fruitful discussions.

Electronic Supplementary Material: Supplementary material (electrode design, equivalent circuit of setup, nanowires grown from tip to tip) is available in the online version of this article at http://dx.doi.org/10.1007/s12274-013-0303-0.

References

[1] Cheng, G.; Siles, P. F.; Bi, F.; Cen, C.; Bogorin, D. F.; Bark, C. W.; Folkman, C. M.; Park, J.-W.; Eom, C.-B.; Medeiros-Ribeiro, G.; et al. Sketched oxide single-electron transistor. *Nat. Nanotechnol.* **2011**, *6*, 343–347.

[2] Blunt, M. O.; Russell, J. C.; Gimenez-Lopez, M. d. C.; Taleb, N.; Lin, X.; Schröder, M.; Champness, N. R.; Beton, P. H. Guest-induced growth of a surface-based supramolecular bilayer. *Nat. Chem.* **2011**, *3*, 74–78.

[3] Wang, D.; Sheriff, B. A.; Heath, J. R. Silicon p-FETs from ultrahigh density nanowire arrays. *Nano Lett.* **2006**, *6*, 1096–1100.

[4] Kuzyk, A. Dielectrophoresis at the nanoscale. *Electrophoresis* **2011**, *32*, 2307–2313.

[5] Melosh, N. A.; Boukai, A.; Diana, F.; Gerardot, B.; Badolato, A.; Petroff, P. M.; Heath, J. R. Ultrahigh-density nanowire lattices and circuits. *Science* **2003**, *300*, 112–115.

[6] Yang, P.; Yan, R.; Fardy, M. Semiconductor nanowire: What's next? *Nano Lett.* **2010**, *10*, 1529–1536.

[7] Mijatovic, D.; Eijkel, J. C. T.; van den Berg, A. Technologies for nanofluidic systems: Top-down vs. bottom-up—A review. *Lab Chip* **2005**, *5*, 492–500.

[8] He, B.; Morrow, T. J.; Keating, C. D. Nanowire sensors for multiplexed detection of biomolecules. *Curr. Opin. Chem. Biol.* **2008**, *12*, 522–528.

[9] Lal, S.; Hafner, J. H.; Halas, N. J.; Link, S.; Nordlander, P. Noble metal nanowires: From plasmon waveguides to passive and active devices. *Acc. Chem. Res.* **2012**, *45*, 1887–1895.

[10] Yogeswaran, U.; Chen, S.-M. A review on the electrochemical sensors and biosensors composed of nanowires as sensing material. *Sensors* **2008**, *8*, 290–313.

[11] Balasubramanian, K. Challenges in the use of 1D nanostructures for on-chip biosensing and diagnostics: A review. *Biosens. Bioelectron.* **2010**, *26*, 1195–204.

[12] Nerowski, A.; Poetschke, M.; Bobeth, M.; Opitz, J.; Cuniberti, G. Dielectrophoretic growth of platinum nanowires: Concentration and temperature dependence of the growth velocity. *Langmuir* **2012**, *28*, 7498–7504.

[13] Pohl, H. A. *Dielectrophoresis: The Behavior of Neutral Matter in Nonuniform Electric Fields*; Cambridge University Press: Cambridge, 1978.

[14] Li, M.; Bhiladvala, R. B.; Morrow, T. J.; Sioss, J. A.; Lew, K.-K.; Redwing, J. M.; Keating, C. D.; Mayer, T. S. Bottom-up assembly of large-area nanowire resonator arrays. *Nat. Nanotechnol.* **2008**, *3*, 88–92.

[15] Papadakis, S.; Hoffmann, J.; Deglau, D.; Chen, A.; Tyagi, P.; Gracias, D. H. Quantitative analysis of parallel nanowire array assembly by dielectrophoresis. *Nanoscale* **2011**, *3*, 1059–1065.

[16] Hermanson, K. D.; Lumsdon, S. O.; Williams, J. P.; Kaler, E. W.; Velev, O. D. Dielectrophoretic assembly of electrically functional microwires from nanoparticle suspensions. *Science* **2001**, *294*, 1082–1086.

[17] Cheng, C.; Gonela, R. K.; Gu, Q.; Haynie, D. T. Self-assembly of metallic nanowires from aqueous solution. *Nano Lett.* **2005**, *5*, 175–178.

[18] La Ferrara, V.; Madathil, A. P.; Mauro, A. D. G. D.; Massera, E.; Polichetti, T.; Rametta, G. The effect of solvent on the morphology of ZnO nanostructure assembly by dielectrophoresis and its device applications. *Electrophoresis* **2012**, *33*, 2086–2093.

[19] Flanders, B. N. Directed electrochemical nanowire assembly: Precise nanostructrue assembly via dendritic solidification. *Mod. Phys. Lett. B* **2012**, *26*, 1130001.

[20] Ranjan, N.; Vinzelberg, H.; Mertig, M. Growing one-dimensional metallic nanowires by dielectrophoresis. *Small* **2006**, *2*, 1490–1496.

[21] Bhatt, K. H.; Velev, O. D. Control and modeling of the dielectrophoretic assembly of on-chip nanoparticle wires. *Langmuir* **2004**, *20*, 467–476.

[22] Gierhart, B. C.; Howitt, D. G.; Chen, S. J.; Smith, R. L.; Collins, S. D. Frequency dependence of gold nanoparticle superassembly by dielectrophoresis. *Langmuir* **2007**, *23*, 12450–12456.

[23] Ozturk, B.; Talukdar, I.; Flanders, B. N. Directed growth of diameter-tunable nanowires. *Nanotechnology* **2007**, *18*, 365302.

[24] Shelimov, B.; Lambert, J. F.; Che, M.; Didillon, B. Application of NMR to interfacial coordination chemistry: A ^{195}Pt NMR study of the interaction of hexachloroplatinic acid aqueous solutions with alumina. *J. Am. Chem. Soc.* **1999**, *121*, 545–556.

[25] Kawasaki, J. K.; Arnold, C. B. Synthesis of latinum dendrites and nanowires via directed electrochemical nanowire assembly. *Nano Lett.* **2011**, *11*, 781–785.

[26] Ciobanas, A. I.; Bejan, A.; Fautrelle, Y. Dendritic solidification morphology viewed from the perspective of constructal theory. *J. Phys. D: Appl. Phys.* **2006**, *39*, 5252–5266.

[27] Marcus, Y. A simple empirical model describing the thermodynamics of hydration of ions of widely varying charges, sizes, and shapes. *Biophys. Chem.* **1994**, *51*, 111–127.

[28] Gierer, A.; Wirtz, K. Molekulare theorie der mikroreibung (Molecular theory of microfriction). *Z. Naturforschg. A* **1953**, *8a*, 532–538.

[29] Laliberté, M. Model for calculating the viscosity of aqueous solutions. *J. Chem. Eng. Data* **2007**, *52*, 321–335.

[30] Trivedi, R.; Lipton, J.; Kurz, W. Effect of growth rate dependent partition coefficient on the dendritic growth in undercooled melts. *Acta Metall.* **1987**, *35*, 965–970.

[31] Thapa, P. S.; Ackerson, B. J.; Grischkowsky, D. R.; Flanders, B. N. Directional growth of metallic and polymeric nanowires. *Nanotechnology* **2009**, *20*, 235307.

[32] Ranjan, N.; Mertig, M.; Cuniberti, G.; Pompe, W. Dielectrophoretic growth of metallic nanowires and microwires: Theory and experiments. *Langmuir* **2010**, *26*, 552–559.

[33] Lumsdon, S. O.; Scott, D. M. Assembly of colloidal particles into microwires using an alternating electric field. *Langmuir* **2005**, *21*, 4874–4880.